ACS Biomaterials SCIENCE & ENGINEERING

pubs.acs.org/journal/abseba

Letter

Homogeneous Distribution of Exogenous Cells onto De-epithelialized Rat Trachea via Instillation of Cell-Loaded Hydrogel

Jiawen Chen, Seyed Mohammad Mir, Meghan R. Pinezich, John D. O'Neill, Brandon A. Guenthart, Matthew Bacchetta, Gordana Vunjak-Novakovic, Sarah X. L. Huang, and Jinho Kim*

Cite This: *ACS Biomater. Sci. Eng.* 2022, 8, 82−88

Read Online

ACCESS | Metrics & More | Article Recommendations | Supporting Information

ABSTRACT: Injured or diseased airway epithelium due to repeated environmental insults or genetic mutations can lead to a functional decline of the lung and incurable lung diseases. Bioengineered airway tissue constructs can facilitate *in vitro* investigation of human lung diseases and accelerate the development of effective therapeutics. Here, we report robust tissue manipulation modalities that allow: (i) selective removal of the endogenous epithelium of *in vitro* cultured airway tissues and (ii) spatially uniform distribution and prolonged cultivation of exogenous cells that are implanted topically onto the denuded airway lumen. Results obtained highlight that our approach to airway tissue manipulation can facilitate controlled removal of the airway epithelium and subsequent homogeneous distribution of newly implanted cells. This study can contribute to the creation of innovative tissue engineering methodologies that can facilitate the treatment of lung diseases, such as cystic fibrosis, primary ciliary dyskinesia, and chronic obstructive pulmonary disease.

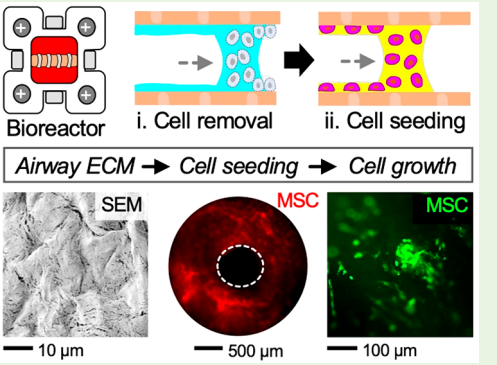

KEYWORDS: *cell replacement, hydrogel, tissue-on-a-chip, bioreactor, imaging, lung disease*

Downloaded via COLUMBIA UNIV on April 28, 2022 at 20:45:29 (UTC).
See https://pubs.acs.org/sharingguidelines for options on how to legitimately share published articles.

The inner lumen of the respiratory tract is lined by the thin epithelium that consists of different cell types, including multiciliated, goblet, club, and basal stem cells.[1,2] These epithelial cells exert defensive barrier functions, such as tight junction formation and mucociliary clearance, that collectively contribute to protection of the underlying airway tissues from inhaled pathogens, allergens, or chemicals.[3] Thus, disruption of the airway epithelium due to repeated environmental insults or genetic defects leads to a functional decline of the lung and devastating lung diseases, such as cystic fibrosis (CF), primary ciliary dyskinesia (PCD), and chronic obstructive pulmonary disease (COPD).[4−9]

To understand pathophysiology of these diseases[10,11] and develop effective therapeutics,[7] different types of *in vitro*[12−15] and animal models[16−19] have been created. Notably, by utilizing recent advances in stem cells, gene editing, biomaterials, and tissue engineering, *in vitro* or *in vivo* cultured airway tissue scaffolds have been established to elucidate underlying molecular or cellular mechanisms associated with different airway diseases.[20−26] In particular, decellularized airway tissues of mice and rats have been used for investigating the survival, proliferation, and differentiation of both healthy and diseased airway epithelial cells by providing tissue-specific niche microenvironments to implanted airway cells.[27−30]

While the bioengineered airway tissues represent promising platforms that can allow high-fidelity disease modeling and efficient drug screening, challenges still remain to further improve reliability and reproducibility of these engineered tissue constructs. In particular, to facilitate incorporation, differentiation, and proliferation of newly implanted cells onto the airway tissue surface, it is important to remove the endogenous epithelium (i.e., de-epithelialization) while keeping the rest of tissue architecture and biochemical components uninterrupted.[27,31] Further, to promote the reconstruction of a fully functional airway epithelium, the implanted new cells must be distributed uniformly and adhered persistently across the de-epithelialized lumen of the airway tissue during their differentiation and proliferation (i.e., re-epithelialization).[32−34]

Here, we report an airway tissue culture system (i.e., airway bioreactor) with which we demonstrated selective removal of the endogenous airway epithelium without disrupting the underlying subepithelial tissue layers. Further, we investigated the spatial distribution of exogenous cells that are seeded topically onto the de-epithelialized tracheal lumen by intra-

Received: August 13, 2021
Accepted: December 1, 2021
Published: December 7, 2021

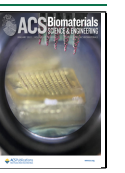

© 2021 American Chemical Society

tracheally instilling a mixture of cells and viscous hydrogel (Figure 1). Using this platform, de-epithelialization of the *ex vivo* rat trachea was achieved by gently exposing the tracheal epithelium to a decellularization solution (e.g., detergent) where the chemically lysed epithelial cells were cleared from the airway during the airway wash with shear flow (Figure 1A). Lab-grown exogenous cells were then topically seeded onto the extracellular matrix (ECM) of the denuded airway lumen by administering a bolus of the cells suspended in the hydrogel solution to promote homogeneous distribution and prolonged retention of the cells on the tissue surface (Figure 1B). In this study, type I collagen was tested as a cell delivery vehicle because it is one of the most abundant components of the lung ECM.[35] Further, mesenchymal stem cells (MSCs) derived from human adipose tissue were used as the model cell to investigate topical cell deposition. We evaluated the cytotoxicity of the denuded rat trachea by cultivating the trachea tissue seeded with MSCs for an extended time period (4 days). The goal of this study was to demonstrate de-epithelialization of the airway epithelium via controlled detergent treatment and subsequent spatially uniform distribution of exogenous cells onto the tissue scaffold.

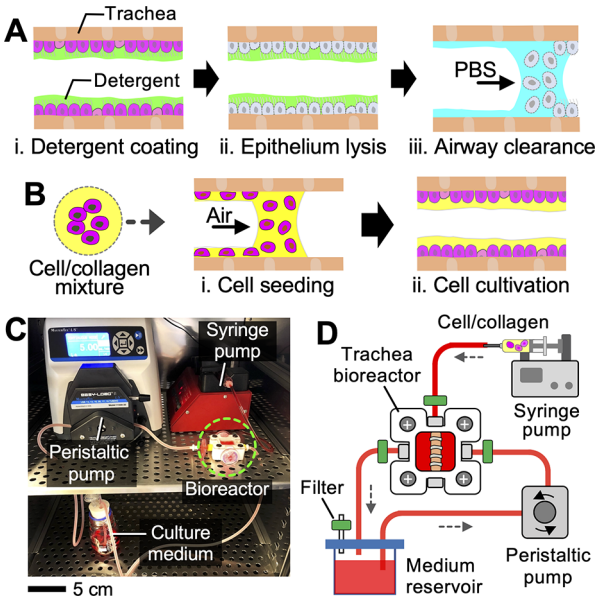

Figure 1. Overview of the epithelium removal and cell implantation. Schematics illustrating (A) epithelium clearance and (B) collagen-assisted cell seeding. (C) Photograph and (D) schematic showing the rat trachea bioreactor.

The rat trachea bioreactor was constructed by integrating a customized trachea culture chamber (dimensions: 2.5 cm × 2.5 cm × 1.5 cm; volume: 9.4 mL), a peristaltic pump (L/S standard digital pump system, Cole-Parmer), a syringe pump (AL-4000, World Precision Instruments), and a culture medium reservoir (Figure 1C,D). The culture chamber, in which explanted rat trachea was cultured during experiments, was created by machining Teflon PTFE plastic using a computer numerical control (CNC) machine (Mini-Mill 3, Minitech). The peristaltic pump circulated the culture medium between the reservoir and the culture chamber (flow rate: 5 mL/min).

The syringe pump delivered a small volume (50 μL) of aqueous solution of sodium dodecyl sulfate (SDS; concentration: 2%; cat. no. 97064-472, VWR) into the rat trachea. Following 20 min of incubation at 37 °C, the lysed epithelium was washed out with 1× PBS solution. A bolus of type I collagen pregel solution (cat. no. 5153, Advanced BioMatrix; volume: 10 μL) carrying MSCs was intratracheally administered to generate a cell-embedded collagen layer on the airway lumen.[34,36,37] Gelation of the collagen pregel occurred within 30 min of incubation at 37 °C. The cell-seeded rat trachea was cultured within the bioreactor up to 4 days to investigate distribution, survival, and proliferation of the implanted cells. All procedures involving the rats were performed in accordance with the animal welfare guideline and regulations of the Institute for Animal Care and Use Committee (IACUC) at Stevens Institute of Technology (Details of experimental procedures and biochemical reagents used in this study are provided in the Supporting Information).

We investigated whether the airway epithelium could be removed from the *in vitro* cultured rat trachea (Figure 2). Following treatment of the trachea with SDS solution and subsequent airway wash (Figure 1A), the trachea tissue was fixed and processed for immunostaining analysis and scanning

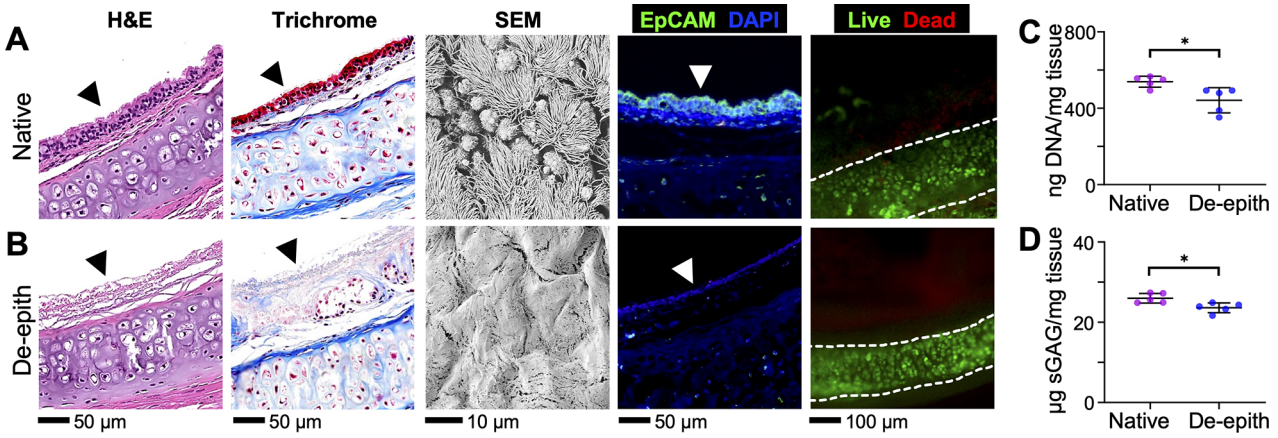

Figure 2. Microscopic analysis of (A) native and (B) de-epithelialized (de-epith) rat tracheas via H&E staining, trichrome staining (cell cytoplasm: pink; nuclei: dark brown; and collagen: blue), SEM imaging, EpCAM (green), DAPI staining (blue), and live/dead staining (green/red). Arrowhead indicates the surface of the tracheal lumen. (C) DNA and (D) sGAG quantification of the rat tracheas before and after de-epithelialization. *$p < 0.05$.

https://doi.org/10.1021/acsbiomaterials.1c01031
ACS Biomater. Sci. Eng. 2022, 8, 82−88

electron microscopy (SEM). In the native rat trachea tissues, the endogenous epithelium and subepithelial tissues were clearly visible in the images obtained via hematoxylin and eosin (H&E), Masson's trichrome, epithelial cellular adhesion molecule (EpCAM), 4′,6-diamidino-2-phenylindole (DAPI), and Movat's pentachrome staining (Figures 2A, S1, and S2).[38,39] On the other hand, the rat trachea treated with SDS solution consistently showed the absence of the epithelial layer (Figure 2B). Notably, the trichrome, pentachrome, and EpCAM staining images revealed that subepithelial tissue layers were well preserved in the de-epithelialized rat trachea. Further, SEM images of the native trachea showed the intact airway epithelium, including multiciliated and goblet cells, lining the tracheal lumen while the airway ECM was exposed with no epithelium presented in the SDS-treated trachea (Figures 2B, S1, and S3). Notably, live/dead staining results showed that the chondrocytes in the cartilage, which are important for maintaining the airway viability, remained intact following the de-epithelialization. To check apoptosis of the chondrocytes, an evaluation of the size of the chondrocyte nuclei was performed via DAPI staining (Figure S4). The chondrocyte nuclei in de-epithelialized tracheas showed a similar size range to that in native tracheas, indicating no obvious apoptosis occurred after de-epithelialization.[40,41] Quantification of DNA showed an 18.2% decrease in DNA content in de-epithelialized tracheas compared to native tracheas (Figure 2C), attributed to the removal of the surface epithelium. Further, nearly 91% of sulfated glycosaminoglycan (sGAG), which is a physiologically important matrix component of cartilage, was preserved following de-epithelialization (Figure 2D). Through a hydroxyproline assay, we confirmed that changes in the total collagen quantity in the tissue was negligible following the treatment. Assuming collagen contains approximately 12% hydroxyproline by mass, we estimated 46.5 and 44.6 μg of collagen in 1 mg of native and de-epithelialized airway tissues, respectively (Figure S5).[42] These results collectively showed the effectiveness of our SDS-based selective de-epithelialization methodology.

We then evaluated the utility of the collagen pregel solution as a cell-delivery vehicle using gelatin-based tubes (diameter: 2 mm) that were used as the airway mimic (Figure 3). In this *in vitro* study, we used fluorescent microparticles (excitation/emission: 488 nm/515 nm; cat. no. F8836, Invitrogen) with 10 μm diameter and 1.06 g/cm^3 density because of their hydrodynamic similarity with cells and easy access. Further, a custom-built laser light sheet microscope (LSM) and GRIN lens imaging system were used to visually inspect the distribution of the particles deposited within the gelatin tube (Figures 3A, S6, and S7).[34] In our LSM, a thin light sheet (thickness: ~5 μm) was created across the tube using a 488 nm laser (cat. no. MDL-D-488, Opto Engine) to obtain fluorescent images of the cross section of the tube interior. A GRIN lens imaging probe (diameter: 500 μm; SELFOC, NSG Group) was inserted directly into the tube to visualize the tube inner surface. As the viscosity of the particle-carrying medium could influence the transport behavior of the particles (e.g., seeding density, spatial distribution),[34,36,37] collagen solutions with different concentrations (0.9, 1.8, and 3 mg/mL) and PBS (control) were prepared in which microparticles were suspended (final particle concentration: 5×10^6 particle/mL).

Following instillation of the particle-carrying collagen pregels or PBS solution (volume: 10 μL, flow rate: 5 mL/min) into the gelatin tubes, the inner surface of each tube was

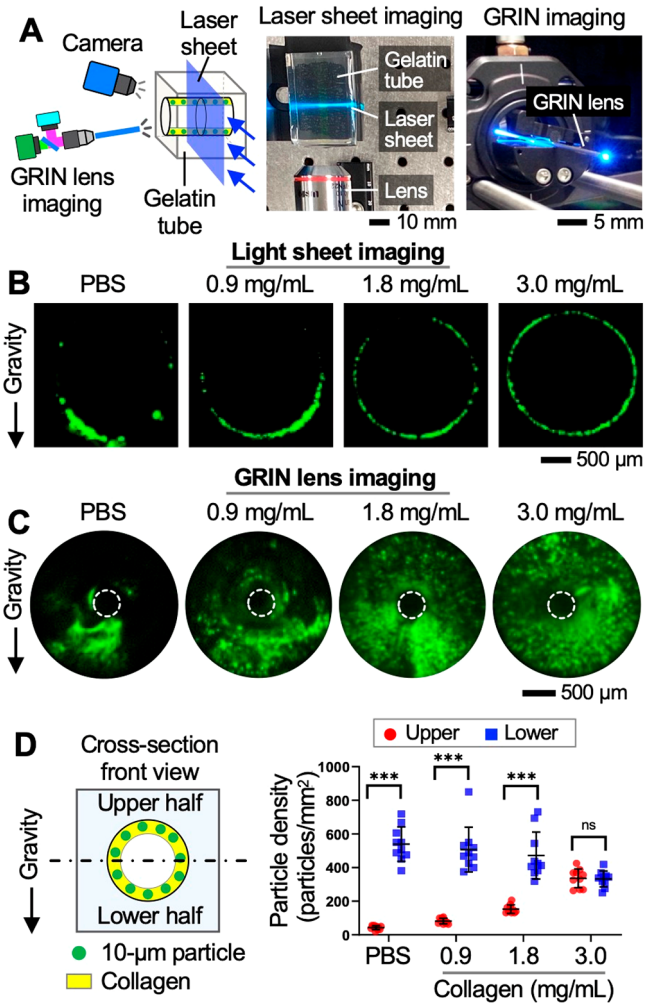

Figure 3. Topical deposition of fluorescent microparticles in a gelatin-based tubular structure. (A) Laser light sheet microscope and GRIN lens imaging system constructed for imaging the interior of the tube. (B, C) Microscopic images of the particles (green) deposited in the tube via PBS and different concentrations of collagens. (D) Particle seeding density measured in upper and lower half of the tube after 30 min of cell seeding. ***$p < 0.001$. ns: not significant.

visualized using our imaging systems. Results showed that when the particles were delivered via PBS, the majority of the particles accumulated onto the lower surface of the tube due to gravity. On the other hand, the increased surface area of the tube was covered by the particles when the particles were delivered via collagen solutions (Figure 3B, C). The density of the particles deposited on the upper and lower half of the tube surfaces was compared via imaging analysis using ImageJ. Notably, the uniformity of the spatial distribution of the deposited particles increased with the concentration of the collagen. As the collagen concentration increased, the difference between the particle seeding density between the upper and lower half surfaces consecutively decreased (i.e., 426 particles/mm^2 for 0.9 mg/mLcollagen vs 4 particles/mm^2 for 3.0 mg/mLcollagen) (Figures 3D and S8).

Using *ex vivo* rat tracheas and fluorescently labeled MSCs (the model cells used in this study), we investigated whether the collagen pregel could promote homogeneous cell distribution onto the de-epithelialized tracheal lumen (Figure 4). As our *in vitro* experiments showed that the collagen pregel

https://doi.org/10.1021/acsbiomaterials.1c01031
ACS Biomater. Sci. Eng. 2022, 8, 82−88

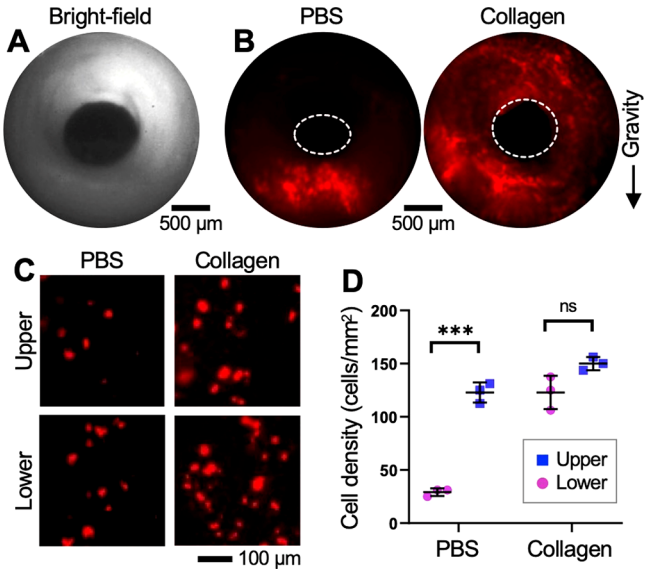

Figure 4. Topical deposition of exogenous cells onto de-epithelialized rat tracheal lumen. (A) Bright-field image of the trachea interior. (B) Fluorescent images of the denuded trachea lumen seeded with MSCs (red) via PBS or collagen. (C) Fluorescent images and (D) cell seeding density obtained in the upper and lower half of the tracheal lumen. ***$p < 0.001$. ns: not significant.

with a 3 mg/mL concentration provided the most uniform particle distribution, we used this collagen concentration in this study. MSCs were labeled with quantum dots (emission wavelength: 655 nm; cat. no. Q21321MP, Thermo Fisher Scientific) and suspended in culture medium (cell concentration: 5×10^6 cells/mL). We then instilled 10 μL of the MSC-loaded collagen into a de-epithelialized rat trachea at a 5 mL/min flow rate and monitored the distribution of the cells on the tracheal lumen using our GRIN lens imaging system (Figure 3). In the bright-field imaging mode, our imaging system clearly showed the interior of the rat trachea (Figure 4A). Consistent with the *in vitro* study, the fluorescently labeled cells that were delivered via collagen remained adhered more uniformly across the lumen compared with those seeded via PBS (control; Figure 4B). Further, the difference in the cell seeding density between the upper (123 cells/mm^2) and lower half of the tube (150 cells/mm^2) was insignificant, highlighting the effectiveness of the collagen-based cell seeding (Figure 4C, D).

Next, we investigated whether the implanted cells by collagen pregel solution could maintain the homogeneous cell distribution during subsequent *in vitro* tissue cultivation and whether the seeded cells survive and proliferate on the de-epithelialized rat tracheal lumen (Figure 5). To improve the visibility of the cells, MSCs were labeled with carboxyfluorescein succinimidyl ester (CFSE) prior to cell seeding. The bioreactor containing de-epithelialized rat tracheas seeded with MSCs was maintained in a cell culture incubator (Cat. No. MCO-20AIC, Panasonic) up to 4 days. During *in vitro* cultivation, the inner space of the trachea was filled with culture medium which was replaced with fresh medium every 24 h. Spatial distributions and shapes of the seeded cells were inspected via fluorescent microscopy following 1 day and 4

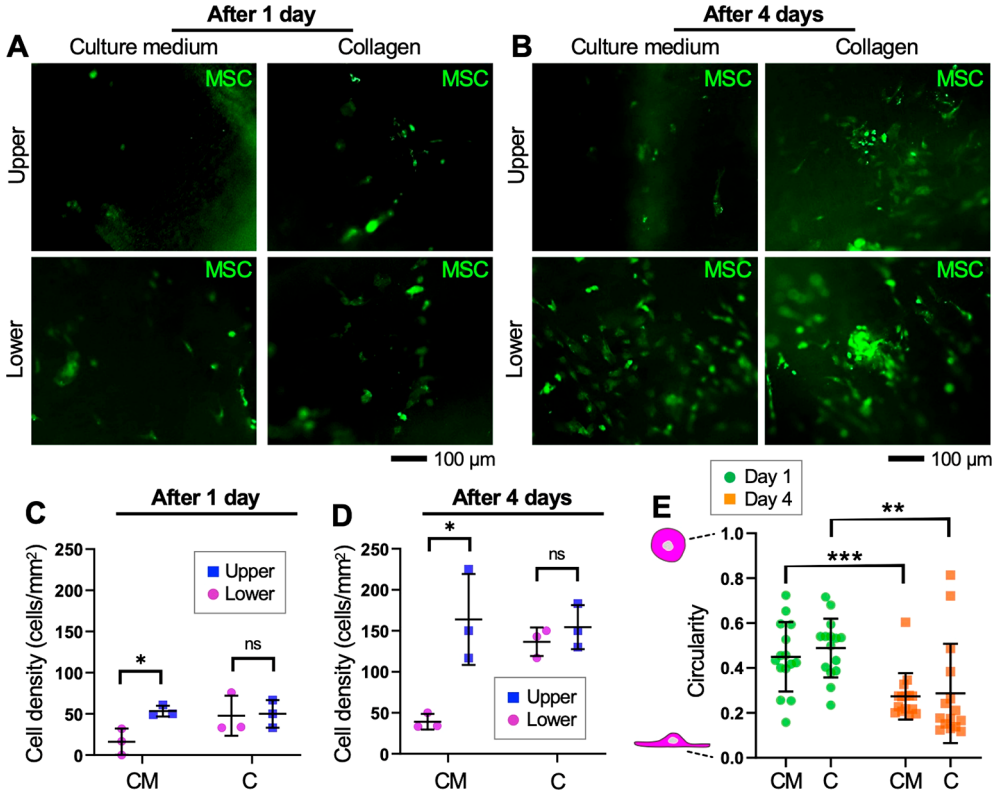

Figure 5. Proliferation of seeded MSCs on the de-epithelialized rat tracheal lumen. Fluorescence images of the tracheas seeded with CFSE-labeled MSCs (green) obtained following (A) 1 day and (B) 4 days of *in vitro* cultivation. Cell densities measured in the upper and lower half of the trachea lumens following (C) 1 day and (D) 4 days of *in vitro* cultivation. (E) Circularity of the seeded cells measured over time. CM: culture medium. C: collagen. *$p < 0.05$. **$p < 0.01$. ***$p < 0.001$. ns: not significant.

https://doi.org/10.1021/acsbiomaterials.1c01031
ACS Biomater. Sci. Eng. 2022, 8, 82−88

days of *in vitro* cultivation of the cell-tissue constructs. The cells seeded via both collagen and culture medium (control) proliferated on the de-epithelialized trachea surface as indicated by the increased number of cells expressing CFSE over time in both the upper and lower half of the tracheal lumen (Figure 5A, B). In the collagen group, however, the difference in the density of the cells between the upper and lower lumens was minimal after 4 days of *in vitro* cultivation (upper surface: 137 cells/mm^2, lower surface: 154 cells/mm^2) (Figure 5C, D). Meanwhile, the cell circularity, which is the ratio of the area to the perimeter of the cells, was determined to quantitatively evaluate the degree of cell engraftment onto the tissue surface (Figure 5E). In both the collagen and culture medium group, the seeded cells displayed a squamous morphology and reduced circularity at day 4, suggesting that the de-epithelialized tracheas were capable of supporting cell engraftment and survival, and the collagen hydrogel did not alter the motility of the implanted cells. Notably, live/dead staining showed that the cells remained viable following hydrogel-based cell seeding (Figure S9). Quantifying the efficiency of the cell delivery is difficult because the number of seeded cells can be largely influenced by different factors in each experiment, such as the surface area of the airway lumen, concentration of the cells mixed in the hydrogel, and speed of the hydrogel instilled into the airway. Thus, in this study, we evaluate the density of the cells deposited and cultured on the de-epithelialized airway lumen (Figures 4 and 5).

In conclusion, we showed that homogeneous spatial distribution and prolonged engraftment of exogenous cells across the luminal surface of the airway can be achieved via instillation of a cell-suspended collagen pregel. Compared with a cell culture medium, the collagen pregel solution facilitated persistent attachment of the cells onto the airway lumen because of its higher viscosity and surface adhesion strength.[34,36,37] One of the main goals of this study was to show that spatially homogeneous cell seeding can be achieved via instillation of the cells suspended in a hydrogel bolus. Accordingly, we showed the benefit of hydrogel-based cell delivery compared with liquid-based delivery in terms of uniform cell distribution following cell seeding. Significantly, the collagen gel created an environment that allowed survival and proliferation of the cells implanted onto the de-epithelialized rat trachea lumen. Further, survival and growth of the implanted cells indicated that the SDS treatment applied to the rat trachea to remove its epithelium did not create a cytotoxic condition for the seeded cells. While MSCs were used as the model cell in this study, future studies that use airway epithelial cells or basal stem cells will further confirm regeneration of the functional epithelium using the collagen-based cell implantation modality. Different hydrogels, such as tissue ECM-derived hydrogels, could be tested as cell delivery vehicles to evaluate the impacts of physical and biochemical properties of the hydrogel. While the adhesion strength of the airway epithelium and MSC cells to the airway ECM can be different, this study highlights the utility of the hydrogel-based cell seeding in initial homogeneous distribution of the instilled cells across the airway lumen. In our cell seeding approach, transport and deposition of the cells will be largely affected by the hydrodynamic and biophysical properties of a hydrogel bolus instilled, such as instillation speed, viscosity, surface tension, and gelation time.[34,36,37]

The approach of collagen-based cell deposition described in this study can provide considerable advantages in the creation of innovative tissue engineering methods for the regeneration of functional airway tissues. Rapid coverage of the de-epithelialized airway surface with newly implanted cells, such as airway basal stem cells,[12,23,43] can accelerate regeneration of the functional epithelium with a reduced risk for contamination of the tissue constructs. Further, growth factors and biochemical reagents that are essential for differentiation of the implanted cells could be added to the collagen pregel prior to cell seeding to modulate cellular activities and responses over time during *in vitro* culture. In addition, because cells are embedded within collagen gel as a cell layer, the *ex vivo* airway can be ventilated with air, providing a more physiologically relevant condition to the *ex vivo* tissue. Our cell replacement technique can be also useful for tissue engineering other organs, such as liver, that require the vasculature network to be preserved during cell replacement procedures. Collectively, our hydrogel-based cell delivery method not only can facilitate the generation of *in vitro* airway tissues but also can inform stem cell replacement therapy by enabling the replacement of the damaged or injured epithelium within the respiratory tract of live patients or donor lungs deemed unsuitable for transplant.[44−46]

■ ASSOCIATED CONTENT

Supporting Information

The Supporting Information is available free of charge at https://pubs.acs.org/doi/10.1021/acsbiomaterials.1c01031.

Supporting materials and methods: gelatin tube fabrication, imaging system construction, rat trachea isolation and de-epithelialization, immunostaining and SEM analysis, DNA and GAG quantification, chondrocyte viability, collagen quantification, bioreactor construction, cell distribution study, cell viability after delivery, cell-tissue cultivation, statistical analysis; pentachrome staining of airway tissues; DAPI staining of airway tissues; DAPI and EpCAM staining of airway tissues; DAPI staining of chondrocytes; collagen quantification; laser sheet microscope; GRIN-lens imaging system; fluorescent particles deposited in gelatin tubes; cell viability assessment (PDF)

■ AUTHOR INFORMATION

Corresponding Author

Jinho Kim − *Department of Biomedical Engineering, Stevens Institute of Technology, Hoboken, New Jersey 07302, United States;* orcid.org/0000-0002-4692-4407; Email: jkim6@stevens.edu

Authors

Jiawen Chen − *Department of Biomedical Engineering, Stevens Institute of Technology, Hoboken, New Jersey 07302, United States*

Seyed Mohammad Mir − *Department of Biomedical Engineering, Stevens Institute of Technology, Hoboken, New Jersey 07302, United States*

Meghan R. Pinezich − *Department of Biomedical Engineering, Columbia University, New York, New York 10032, United States*

John D. O'Neill − *Department of Cell Biology, State University of New York Downstate Medical Center, Brooklyn, New York 11203, United States*

Brandon A. Guenthart − *Department of Cardiothoracic Surgery, Stanford University, Stanford, California 94305, United States*
Matthew Bacchetta − *Department of Thoracic Surgery, Vanderbilt University, Nashville, Tennessee 37232, United States*
Gordana Vunjak-Novakovic − *Department of Biomedical Engineering, Columbia University, New York, New York 10032, United States;* orcid.org/0000-0002-9382-1574
Sarah X. L. Huang − *Center for Stem Cell and Regenerative Medicine, University of Texas Health Science Center, Houston, Texas 77030, United States*

Complete contact information is available at: https://pubs.acs.org/10.1021/acsbiomaterials.1c01031

Author Contributions

The manuscript was written through contributions of all authors. All authors approved the final version of the manuscript.

Funding

This research has been supported in part by American Thoracic Society Foundation Research Program and Research Grants from New Jersey Health Foundation provided to J.K.

Notes

The authors declare no competing financial interest.

■ ACKNOWLEDGMENTS

The authors would like to thank Drs. Tsengming (Alex) Chou and Matthew Libera, and Mr. Xinpei Wu at Stevens Laboratory for Multiscale Imaging (LMSI) for their assistance with SEM imaging of the tissue samples.

■ ABBREVIATIONS

SDS, sodium dodecyl sulfate; PBS, phosphate buffered saline; SEM, scanning electron microscopy; EpCAM, epithelial cellular adhesion molecule; MSC, mesenchymal stem cell; CFSE, carboxyfluorescein succinimidyl ester; ECM, extracellular matrix

■ REFERENCES

(1) Li, F.; He, J.; Wei, J.; Cho, W. C.; Liu, X. Diversity of epithelial stem cell types in adult lung. *Stem Cells Int.* **2015**, *2015*, 728307.
(2) Franks, T. J.; Colby, T. V.; Travis, W. D.; Tuder, R. M.; Reynolds, H. Y.; Brody, A. R.; Cardoso, W. V.; Crystal, R. G.; Drake, C. J.; Engelhardt, J.; Frid, M.; Herzog, E.; Mason, R.; Phan, S. H.; Randell, S. H.; Rose, M. C.; Stevens, T.; Serge, J.; Sunday, M. E.; Voynow, J. A.; Weinstein, B. M.; Whitsett, J.; Williams, M. C. Resident cellular components of the human lung: current knowledge and goals for research on cell phenotyping and function. *Proc. Am. Thorac. Soc.* **2008**, *5* (7), 763−766.
(3) Crystal, R. G.; Randell, S. H.; Engelhardt, J. F.; Voynow, J.; Sunday, M. E. Airway epithelial cells: current concepts and challenges. *Proc. Am. Thorac. Soc.* **2008**, *5* (7), 772−777.
(4) Trinh, N. T.; Bardou, O.; Prive, A.; Maille, E.; Adam, D.; Lingee, S.; Ferraro, P.; Desrosiers, M. Y.; Coraux, C.; Brochiero, E. Improvement of defective cystic fibrosis airway epithelial wound repair after CFTR rescue. *Eur. Respir. J.* **2012**, *40* (6), 1390−1400.
(5) Roscioli, E.; Hamon, R.; Lester, S. E.; Jersmann, H. P. A.; Reynolds, P. N.; Hodge, S. Airway epithelial cells exposed to wildfire smoke extract exhibit dysregulated autophagy and barrier dysfunction consistent with COPD. *Respir. Res.* **2018**, *19* (1), 234.
(6) Horani, A.; Ferkol, T. W. Advances in the Genetics of Primary Ciliary Dyskinesia: Clinical Implications. *Chest* **2018**, *154* (3), 645−652.
(7) Mianne, J.; Ahmed, E.; Bourguignon, C.; Fieldes, M.; Vachier, I.; Bourdin, A.; Assou, S.; De Vos, J. Induced Pluripotent Stem Cells for Primary Ciliary Dyskinesia Modeling and Personalized Medicine. *Am. J. Respir. Cell Mol. Biol.* **2018**, *59* (6), 672−683.
(8) Cohen-Cymberknoh, M.; Kerem, E.; Ferkol, T.; Elizur, A. Airway inflammation in cystic fibrosis: molecular mechanisms and clinical implications. *Thorax* **2013**, *68* (12), 1157−1162.
(9) Sidhaye, V. K.; Koval, M. *Lung Epithelial Biology in the Pathogenesis of Pulmonary Disease*; Academic Press: 2017.
(10) Gosens, R.; Zaagsma, J.; Meurs, H.; Halayko, A. J. Muscarinic receptor signaling in the pathophysiology of asthma and COPD. *Respir. Res.* **2006**, *7* (1), 73.
(11) Grubb, B. R.; Boucher, R. C. Pathophysiology of gene-targeted mouse models for cystic fibrosis. *Physiol. Rev.* **1999**, *79* (1), S193−214.
(12) Hawkins, F. J.; Suzuki, S.; Beermann, M. L.; Barilla, C.; Wang, R.; Villacorta-Martin, C.; Berical, A.; Jean, J. C.; Le Suer, J.; Matte, T.; Simone-Roach, C.; Tang, Y.; Schlaeger, T. M.; Crane, A. M.; Matthias, N.; Huang, S. X. L.; Randell, S. H.; Wu, J.; Spence, J. R.; Carraro, G.; Stripp, B. R.; Rab, A.; Sorsher, E. J.; Horani, A.; Brody, S. L.; Davis, B. R.; Kotton, D. N. Derivation of Airway Basal Stem Cells from Human Pluripotent Stem Cells. *Cell Stem Cell* **2021**, *28* (1), 79−95.
(13) Haswell, L. E.; Hewitt, K.; Thorne, D.; Richter, A.; Gaca, M. D. Cigarette smoke total particulate matter increases mucous secreting cell numbers in vitro: a potential model of goblet cell hyperplasia. *Toxicol. In Vitro* **2010**, *24* (3), 981−987.
(14) Plebani, R.; Potla, R.; Soong, M.; Bai, H.; Izadifar, Z.; Jiang, A.; Travis, R. N.; Belgur, C.; Dinis, A.; Cartwright, M. J.; Prantil-Baun, R.; Jolly, P.; Gilpin, S. E.; Romano, M.; Ingber, D. E. Modeling Pulmonary Cystic Fibrosis in a Human Lung Airway-on-a-chip. *J. Cystic Fibrosis* **2021**, DOI: 10.1016/j.jcf.2021.10.004.
(15) McCauley, K. B.; Hawkins, F.; Serra, M.; Thomas, D. C.; Jacob, A.; Kotton, D. N. Efficient Derivation of Functional Human Airway Epithelium from Pluripotent Stem Cells via Temporal Regulation of Wnt Signaling. *Cell Stem Cell* **2017**, *20* (6), 844−857.
(16) Ostrowski, L. E.; Yin, W.; Rogers, T. D.; Busalacchi, K. B.; Chua, M.; O'Neal, W. K.; Grubb, B. R. Conditional deletion of dnaic1 in a murine model of primary ciliary dyskinesia causes chronic rhinosinusitis. *Am. J. Respir. Cell Mol. Biol.* **2010**, *43* (1), 55−63.
(17) Snouwaert, J. N.; Brigman, K. K.; Latour, A. M.; Malouf, N. N.; Boucher, R. C.; Smithies, O.; Koller, B. H. An animal model for cystic fibrosis made by gene targeting. *Science* **1992**, *257* (5073), 1083−1088.
(18) Churg, A.; Tai, H.; Coulthard, T.; Wang, R.; Wright, J. L. Cigarette smoke drives small airway remodeling by induction of growth factors in the airway wall. *Am. J. Respir. Crit. Care Med.* **2006**, *174* (12), 1327−1334.
(19) Wright, J. L.; Cosio, M.; Churg, A. Animal models of chronic obstructive pulmonary disease. *Am. J. Physiol.: Lung Cell. Mol. Physiol.* **2008**, *295* (1), L1−15.
(20) Goldman, M. J.; Yang, Y.; Wilson, J. M. Gene therapy in a xenograft model of cystic fibrosis lung corrects chloride transport more effectively than the sodium defect. *Nat. Genet.* **1995**, *9* (2), 126−131.
(21) Chen, Y. W.; Huang, S. X.; de Carvalho, A.; Ho, S. H.; Islam, M. N.; Volpi, S.; Notarangelo, L. D.; Ciancanelli, M.; Casanova, J. L.; Bhattacharya, J.; Liang, A. F.; Palermo, L. M.; Porotto, M.; Moscona, A.; Snoeck, H. W. A three-dimensional model of human lung development and disease from pluripotent stem cells. *Nat. Cell Biol.* **2017**, *19* (5), 542−549.
(22) Nossa, R.; Costa, J.; Cacopardo, L.; Ahluwalia, A. Breathing in vitro: Designs and applications of engineered lung models. *J. Tissue Eng.* **2021**, *12*, 1−28.
(23) Huang, S. X.; Islam, M. N.; O'Neill, J.; Hu, Z.; Yang, Y. G.; Chen, Y. W.; Mumau, M.; Green, M. D.; Vunjak-Novakovic, G.; Bhattacharya, J.; Snoeck, H. W. Efficient generation of lung and airway epithelial cells from human pluripotent stem cells. *Nat. Biotechnol.* **2014**, *32* (1), 84−91.

(24) Lodes, N.; Seidensticker, K.; Perniss, A.; Nietzer, S.; Oberwinkler, H.; May, T.; Walles, T.; Hebestreit, H.; Hackenberg, S.; Steinke, M. Investigation on Ciliary Functionality of Different Airway Epithelial Cell Lines in Three-Dimensional Cell Culture. *Tissue Eng., Part A* **2020**, *26* (7−8), 432−440.
(25) Gkatzis, K.; Taghizadeh, S.; Huh, D.; Stainier, D. Y. R.; Bellusci, S. Use of three-dimensional organoids and lung-on-a-chip methods to study lung development, regeneration and disease. *Eur. Respir. J.* **2018**, *52* (5), 1800876.
(26) Steinke, M.; Gross, R.; Walles, H.; Gangnus, R.; Schutze, K.; Walles, T. An engineered 3D human airway mucosa model based on an SIS scaffold. *Biomaterials* **2014**, *35* (26), 7355−7362.
(27) Dorrello, N. V.; Guenthart, B. A.; O'Neill, J. D.; Kim, J.; Cunningham, K.; Chen, Y. W.; Biscotti, M.; Swayne, T.; Wobma, H. M.; Huang, S. X. L.; Snoeck, H. W.; Bacchetta, M.; Vunjak-Novakovic, G. Functional vascularized lung grafts for lung bioengineering. *Sci. Adv.* **2017**, *3* (8), No. e1700521.
(28) Zang, M.; Zhang, Q.; Chang, E. I.; Mathur, A. B.; Yu, P. Decellularized tracheal matrix scaffold for tracheal tissue engineering: in vivo host response. *Plast. Reconstr. Surg.* **2013**, *132* (4), 549e−559e.
(29) Cortiella, J.; Niles, J.; Cantu, A.; Brettler, A.; Pham, A.; Vargas, G.; Winston, S.; Wang, J.; Walls, S.; Nichols, J. E. Influence of acellular natural lung matrix on murine embryonic stem cell differentiation and tissue formation. *Tissue Eng., Part A* **2010**, *16* (8), 2565−2580.
(30) Kutten, J. C.; McGovern, D.; Hobson, C. M.; Luffy, S. A.; Nieponice, A.; Tobita, K.; Francis, R. J.; Reynolds, S. D.; Isenberg, J. S.; Gilbert, T. W. Decellularized tracheal extracellular matrix supports epithelial migration, differentiation, and function. *Tissue Eng., Part A* **2015**, *21* (1−2), 75−84.
(31) Crapo, P. M.; Gilbert, T. W.; Badylak, S. F. An overview of tissue and whole organ decellularization processes. *Biomaterials* **2011**, *32* (12), 3233−3243.
(32) Ott, H. C.; Clippinger, B.; Conrad, C.; Schuetz, C.; Pomerantseva, I.; Ikonomou, L.; Kotton, D.; Vacanti, J. P. Regeneration and orthotopic transplantation of a bioartificial lung. *Nat. Med.* **2010**, *16* (8), 927−933.
(33) Petersen, T. H.; Calle, E. A.; Zhao, L.; Lee, E. J.; Gui, L.; Raredon, M. B.; Gavrilov, K.; Yi, T.; Zhuang, Z. W.; Breuer, C.; Herzog, E.; Niklason, L. E. Tissue-engineered lungs for in vivo implantation. *Science* **2010**, *329* (5991), 538−541.
(34) Kim, J.; Guenthart, B.; O'Neill, J. D.; Dorrello, N. V.; Bacchetta, M.; Vunjak-Novakovic, G. Controlled delivery and minimally invasive imaging of stem cells in the lung. *Sci. Rep.* **2017**, *7* (1), 13082.
(35) Bateman, E. D.; Turner-Warwick, M.; Adelmann-Grill, B. C. Immunohistochemical study of collagen types in human foetal lung and fibrotic lung disease. *Thorax* **1981**, *36* (9), 645−653.
(36) Kim, J.; O'Neill, J. D.; Dorrello, N. V.; Bacchetta, M.; Vunjak-Novakovic, G. Targeted delivery of liquid microvolumes into the lung. *Proc. Natl. Acad. Sci. U. S. A.* **2015**, *112* (37), 11530−11535.
(37) Kim, J.; O'Neill, J. D.; Vunjak-Novakovic, G. Rapid retraction of microvolume aqueous plugs traveling in a wettable capillary. *Appl. Phys. Lett.* **2015**, *107* (14), 144101.
(38) Leonard, A. K.; Loughran, E. A.; Klymenko, Y.; Liu, Y.; Kim, O.; Asem, M.; McAbee, K.; Ravosa, M. J.; Stack, M. S. Methods for the visualization and analysis of extracellular matrix protein structure and degradation. *Methods Cell Biol.* **2018**, *143*, 79−95.
(39) Movat, H. Z. Demonstration of all connective tissue elements in a single section; pentachrome stains. *AMA Arch. Pathol.* **1955**, *60* (3), 289−295.
(40) Mandelkow, R.; Gumbel, D.; Ahrend, H.; Kaul, A.; Zimmermann, U.; Burchardt, M.; Stope, M. B. Detection and Quantification of Nuclear Morphology Changes in Apoptotic Cells by Fluorescence Microscopy and Subsequent Analysis of Visualized Fluorescent Signals. *Anticancer Res.* **2017**, *37* (5), 2239−2244.
(41) Ehlken, H.; Kondylis, V.; Heinrichsdorff, J.; Ochoa-Callejero, L.; Roskams, T.; Pasparakis, M. Hepatocyte IKK2 protects Mdr2−/− mice from chronic liver failure. *PLoS One* **2011**, *6* (10), No. e25942.
(42) Xing, Q.; Yates, K.; Tahtinen, M.; Shearier, E.; Qian, Z.; Zhao, F. Decellularization of fibroblast cell sheets for natural extracellular matrix scaffold preparation. *Tissue Eng., Part C* **2015**, *21* (1), 77−87.
(43) Huang, S. X.; Green, M. D.; de Carvalho, A. T.; Mumau, M.; Chen, Y. W.; D'Souza, S. L.; Snoeck, H. W. The in vitro generation of lung and airway progenitor cells from human pluripotent stem cells. *Nat. Protoc.* **2015**, *10* (3), 413−425.
(44) Hozain, A. E.; O'Neill, J. D.; Pinezich, M. R.; Tipograf, Y.; Donocoff, R.; Cunningham, K. M.; Tumen, A.; Fung, K.; Ukita, R.; Simpson, M. T.; Reimer, J. A.; Ruiz, E. C.; Queen, D.; Stokes, J. W.; Cardwell, N. L.; Talackine, J.; Kim, J.; Snoeck, H. W.; Chen, Y. W.; Romanov, A.; Marboe, C. C.; Griesemer, A. D.; Guenthart, B. A.; Bacchetta, M.; Vunjak-Novakovic, G. Xenogeneic cross-circulation for extracorporeal recovery of injured human lungs. *Nat. Med.* **2020**, *26* (7), 1102−1113.
(45) O'Neill, J. D.; Guenthart, B. A.; Kim, J.; Chicotka, S.; Queen, D.; Fung, K.; Marboe, C.; Romanov, A.; Huang, S. X. L.; Chen, Y. W.; Snoeck, H. W.; Bacchetta, M.; Vunjak-Novakovic, G. Cross-circulation for extracorporeal support and recovery of the lung. *Nat. Biomed. Eng.* **2017**, *1* (3), 1−15.
(46) Guenthart, B. A.; O'Neill, J. D.; Kim, J.; Fung, K.; Vunjak-Novakovic, G.; Bacchetta, M. Cell replacement in human lung bioengineering. *J. Heart Lung Transplant.* **2019**, *38* (2), 215−224.

https://doi.org/10.1021/acsbiomaterials.1c01031
ACS Biomater. Sci. Eng. 2022, 8, 82−88